Micellar drug delivery vehicles formed from amphiphilic block copolymers bearing photo-cross-linkable cyclopentenone side groups

Polymer Chemistry

ROYAL SOCIETY OF CHEMISTRY

PAPER

View Article Online
View Journal | View Issue

Cite this: *Polym. Chem.*, 2022, **13**, 4832

Micellar drug delivery vehicles formed from amphiphilic block copolymers bearing photo-cross-linkable cyclopentenone side groups†

Jules Stouten,[a] Nick Sijstermans,[a,b] Joanna Babilotte,[c] Andrij Pich,[a,d,e] Lorenzo Moroni[c] and Katrien V. Bernaerts*[a]

Amphiphilic block copolymers are of specific interest in the field of nanomedicine, and are used to encapsulate hydrophobic drugs for targeted drug delivery. To improve micellar stability in highly diluted conditions, cross-linkable functional groups can be incorporated in the polymer backbone to covalently link the block copolymers and create nanogels. In this work, we propose the use of a poly(oligo(ethylene glycol) methyl ether acrylate) macro-RAFT agent for the controlled polymerization of 4-oxocyclopentenyl acrylate (4CPA) and lauryl acrylate to obtain amphiphilic block copolymers. The cyclopentenone side groups belonging to the 4CPA monomer are able to dimerize under illumination with UV light, resulting in core cross-linked assemblies. A series of block copolymers containing different hydrophilic and hydrophobic block lengths were synthesized. The block copolymers were able to self-assemble after direct dissolution in water to form micellar structures. However, more defined, smaller, and spherical micelles of between 29 and 161 nm were obtained by producing them *via* a solvent exchange method. The micellar cores were cross-linked using UV irradiation and remained stable in organic solvent where the unmodified micelles dissociated and formed smaller assemblies. The drug loading capacity was firstly investigated using the model drug probes pyrene and Nile red. The most promising block copolymer was loaded with doxorubicin (DOX) with a loading content of 23.8%. *In vitro* release studies showed a delayed DOX release from the UV cross-linked micelles. Furthermore, the release was accelerated at lower pH. Cell viability essays of the DOX loaded micelles confirmed the relevance of the synthesized block copolymers as drug delivery vehicles by showing high cytotoxicity towards breast adenocarcinoma cells. The same non-loaded micelles showed low cytotoxicity at the targeted concentrations towards mouse fibroblast cells.

Received 16th May 2022,
Accepted 2nd August 2022

DOI: 10.1039/d2py00631f

rsc.li/polymers

Introduction

Amphiphilic block copolymers have been widely investigated in the field of nanotechnology and biomedical engineering.[1] Upon introduction in aqueous medium, the incompatible hydrophobic blocks cause the macromolecule to self-assemble into organized structures to reduce the overall free energy. Compared to small surfactant molecules, amphiphilic block copolymers have a low critical aggregation concentration (CAC), and improved micellar stability.[2] Therefore, they can serve as

[a]*Aachen-Maastricht Institute for Biobased Materials (AMIBM), Faculty of Science and Engineering, Maastricht University, Brightlands Chemelot Campus, Urmonderbaan 22, 6167 RD Geleen, The Netherlands.*
E-mail: katrien.bernaerts@maastrichtuniversity.nl; Tel: +31 433882636
[b]*Zuyd University of Applied Science, Faculty of Beta Sciences and Technology, Nieuw Eyckholt 300, 6419 DJ Heerlen, The Netherlands*
[c]*Complex Tissue Regeneration department, MERLN Institute for Technology-Inspired Regenerative Medicine, Maastricht University, Maastricht, The Netherlands*
[d]*DWI Leibniz-Institute for Interactive Materials, Aachen 52056, Germany*
[e]*Institute of Technical and Macromolecular Chemistry (ITMC), RWTH Aachen University, Aachen 52074, Germany*

†Electronic supplementary information (ESI) available: ^{1}H NMR spectrum of $POEGA_{19}$ macro-RAFT agent. Overlay of the GPC traces of POEGA macro-RAFT agents. Jaacks plots of the 4CPA, LA copolymerization reactions. MALDI-ToF-MS spectra of POEGA macro-RAFT agents and block copolymers. DOSY spectra of POEGA macro-RAFT agents and block copolymer. Overview of critical aggregation concentration results for POEGA macro-RAFT agents and corresponding block copolymers. DLS results of the block copolymer assemblies in water. DLS results displaying the difference between method of micelle formation and stability of the micelles after long-term storage. DSC traces of the unmodified and UV cross-linked micelles from $POEGA_{19}$-HB_{50}. Photograph of the Nile red and pyrene loaded micellar solutions. Overlay of the UV-Vis spectra of model drug loaded micelles and control samples in methanol. Overview of the encapsulation efficiency for the block copolymer model drug loading experiments. DLC and size of Nile red loaded micelles. Photograph of DOX loaded cross-linked and non-cross-linked micellar solutions. Photographs of cells during cell viability essay. See DOI: https://doi.org/10.1039/d2py00631f

drug delivery vehicles for hydrophobic drugs by encapsulating the drug and allowing transportation through the body.[3]

Since micelle formation is a reversible process, a commonly faced problem is the premature disintegration, or instability of the micellar structures.[4] Strong dilution or introduction in a different solvent brings the block copolymers in a state where they are more likely to exist as unimers and not in organized micellar structures. One way to tune the stability is to change hydrophilic and hydrophobic block lengths. Typically, a decrease in the CAC can be expected as a result of increasing molecular weight and hydrophobic-to-hydrophilic block length ratio.[2,5] This in turn, can also affect other properties of the resulting micellar structures such as size, shape, and drug loading capacity.[6] Furthermore, for block copolymers with relatively long hydrophobic chains, reaching the thermodynamic equilibrium of micelle formation occurs on a much longer timescale compared to small molecule surfactants. Therefore, the size and shape of the micelles can be highly dependent on the method used for preparation.[3] Another way to stop the reversible micelle formation process is covalent cross-linking between the block copolymer chains to freeze the self-assembled state and improve micellar stabilization.[7]

Core cross-linking of the polymeric micelles retains the micelle structure in dilute conditions and in solvents, avoiding dissociation into unimers. Core cross-linking is straightforward and can be achieved through addition of cross-linkers following micelle formation. This raises concerns regarding the transport of the cross-linker to the micelle core. A more facile method is self-cross-linking of functional groups present on the polymer backbone of the associating (or non-soluble) block. In this way, cross-linking can be induced by external stimuli such as UV light and avoids the addition, and removal of potentially hazardous cross-linker residues. Furthermore, cross-linking can be performed at a wide range of micellar concentrations.

Previous studies on UV-cross-linkable block copolymer micelles have reported the use of pendent functionality including cinnamoyl,[8,9] coumarin,[10,11] anthracene,[12] benzophenone,[13] tetrazole,[14] and thymine[15,16] groups.[17] Another monomer that is able to dimerize *via* [2 + 2] photocyclodimerization under UV light is 4-oxocyclopentenyl acrylate (4CPA) (Fig. 1b).[18] 4CPA is a promising monomer of interest due to the scalable and renewable synthesis of its precursor 4-hydroxycyclopentenone in flow using water as the main solvent, or under supercritical water conditions.[18–20] Amphiphilic block copolymers based on 4CPA for drug delivery applications have not yet been produced, and are therefore an interesting subject of investigation to expand the scope of photo curable polymers in the field of self-assembly. Furthermore, the afore mentioned studies on the synthesis and self-assembly of UV curable amphiphilic block-copolymers, did not include a thorough investigation towards the effects of the individual block lengths on the amphiphilic properties, self-assembly process, and drug loading content. Studies towards the loading and release of therapeutic drugs such as doxorubicin (DOX), and the *in vitro* cytotoxicity of polymers bearing UV-cross-linkable groups are also often lacking.

In this work, we aim to explore the use of 4CPA in core cross-linked amphiphilic block copolymers synthesized by RAFT polymerization. RAFT controlled polymerization is an outstanding and facile method for synthesizing well-defined block copolymers, while maintaining control over the individual block length.[21–23] As a hydrophilic block and simultaneously macro-RAFT agent, poly(oligo(ethylene glycol) methyl ether acrylate) (POEGA) was used (Fig. 1a). Block copolymers containing PEG hydrophilic segments are well established in drug delivery applications. They result in stable drug delivery carriers that are highly biocompatible and resistant to protein adsorption.[5,24] Similarly to PEG, POEGA synthesized by RAFT polymerization bearing trithiocarbonate end groups, displays good biocompatibility[25,26] Herein, POEGA blocks of various lengths were employed in a RAFT polymerization with a mixture of lauryl acrylate (LA) and 4CPA in a 70 : 30 mol%

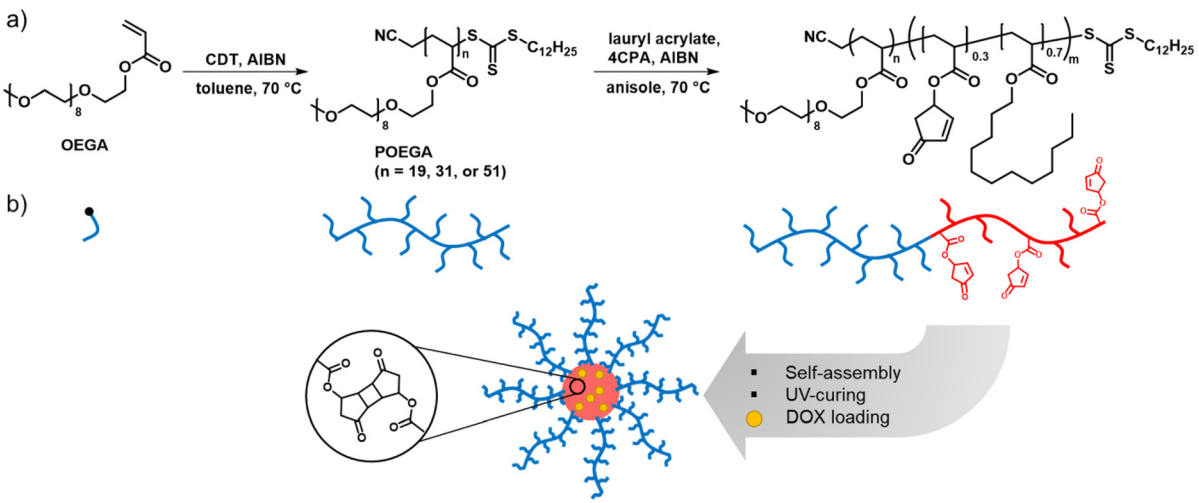

Fig. 1 (a) Synthesis of the POEGA macro-RAFT agent and 4CPA based block copolymers, (b) a schematic representation of the self-assembled and UV-cured micelles.

ratio to function as the hydrophobic block. The renewable LA was chosen because its hydrophobic character promotes micellar formation by means of hydrophobic interactions to form well-defined micellar aggregates.[27] Decoration of the hydrophobic block with long alkyl chains has been reported to lead to low CAC values.[28] Encapsulation with the model probes pyrene and Nile red will resolve the most promising block copolymer structure resulting in micelles with a small size and capable of high drug encapsulation. Furthermore, the cytotoxicity of these UV-cross-linkable micelles will be evaluated before and after loading with DOX indicating the potential for application as drug delivery vehicles. DOX is a hydrophobic therapeutic drug used to treat different types of cancer, including breast cancer.[29]

Experimental

Materials

Azobisisobutyronitrile (AIBN, Sigma-Aldrich) was recrystallized from methanol prior to use. Oligo(ethylene glycol) methyl ether acrylate (OEGA, average M_n of 480 g mol^{-1}, Sigma-Aldrich), and lauryl acrylate (LA, >98.0%, TCI) were passed over an alumina columnto remove the inhibitor and stored at −20 °C. 4-Oxocyclopent-2-ene-1-yl acrylate (4CPA) was synthesized according to a procedure mentioned in the literature and stored at −20 °C.[18] Cyanomethyl dodecyl trithiocarbonate (CDT) was synthesized according to a procedure reported previously and stored at 4 °C.[30] *trans*-2-[3-(4-*tert*-Butylphenyl)-2-methyl-2-propenylidene]malononitrile (DCTB, ≥96%, Sigma-Aldrich), triethylamine (TEA, ≥99%, Sigma-Aldrich), sodium trifluoroacetate (KTFA, 98%, Sigma-Aldrich), 1,3,5-trioxane (≥99%, Sigma-Aldrich), naphthalene (99.5%, Sigma-Aldrich), pyrene (>99%, Alfa-Aesar), Nile red (TCI), doxorubicin hydrochloride (DOX-HCl, >95.0%, TCI), D_2O (99.8 atom% D, Acros organics), and $CDCl_3$ (99.8 atom% D, Cambridge Isotope Laboratories) were used as received. All other solvents were obtained from Biosolve and were used as received. Regenerated cellulose dialysis membranes with a molecular weight cut-off of 1 kDa were purchased from Fisher Scientific.

Synthesis of poly(oligo(ethylene glycol) methyl ether acrylate) (POEGA) macro-RAFT agent

Three POEGA macro-RAFT agents with different block lengths were synthesized; these are summarized in Table 1. The syntheses were all performed in the same way except the ratios between monomer and RAFT agent were varied to aim for different block lengths. In an exemplary synthesis, a 100 mL Schlenk flask equipped with magnetic stirrer was charged with oligo(ethylene glycol) methyl ether acrylate (OEGA) (15.0 g, 31.25 mmol, 220 eq.), CDT (451 mg, 1.42 mmol, 10 eq.), AIBN (23.3 mg, 0.142 mmol, 1 eq.), trioxane (130 mg, as internal standard), and toluene (42 mL, monomer concentration was 30 wt%). The mixture was degassed by sparging with nitrogen for at least 30 minutes. The flask was sealed with a nitrogen filled balloon and the polymerization was started by placing the flask in a 70 °C oil bath. The monomer conversion was followed by ^{1}H NMR spectroscopy by comparing the acrylate resonances with the trioxane resonances at 5.20 ppm. The reaction was stopped after 5 hours. The polymer was precipitated three times in hexane and dried in a vacuum oven at 40 °C overnight. The ^{1}H NMR spectrum of the final polymer in $CDCl_3$ is shown in Fig. S1.† The degree of polymerization was calculated by comparing the RAFT agent end-group resonance at 0.86 ppm with the POEGA resonance at 4.14 ppm. Yield: 14.9 g of a yellow viscous liquid (95%).

Synthesis of block copolymers

Using the three POEGA macro-RAFT agents, a series of nine block copolymers were synthesized with different hydrophobic block lengths. The molar feed ratio of 4CPA : LA was kept at 3 : 7. In an exemplary synthesis ($POEGA_{19}$-HB_{16}), a 25 mL Schlenk flask equipped with magnetic stirrer was charged with 4CPA (500 mg, 3.29 mmol, 6 eq.), LA (1844 mg, 7.67 mmol, 14 eq.), AIBN (18 mg, 0.11 mmol, 0.2 eq.), $POEGA_{19}$ macro-RAFT agent (5096 mg, 0.54 mmol, 1 eq.), naphthalene (60 mg, as GC-FID internal standard), and anisole (3.51 mL, monomer concentration was 40 wt%). The mixture was degassed by at least three consecutive freeze–pump–thaw cycles. After the last cycle, the flask was filled with nitrogen, and the mixture thoroughly homogenized. The flask was sealed with a nitrogen filled balloon and the polymerization was started by placing the flask in a 70 °C oil bath. The reaction was continued until the monomer conversion plateaued according to GC-FID analysis. After the reaction was finished, the flask was cooled to room temperature and the polymer purified by dialysis against methanol in a regenerated cellulose dialysis membrane with a molecular weight cutoff of 1 kDa. The polymer was dried overnight in a vacuum oven at 40 °C and then stored at 4 °C. Yield: 3.89 g of a yellow viscous liquid (52%).

The monomer ratios in the purified polymer were determined by comparing the resonances of 4CPA, OEGA and LA at 7.58, 3.65, and 0.88 ppm, respectively. After correction for the

Table 1 Characteristics of the synthesized POEGA macro-RAFT agents

	Molar feed ratio									
Polymer	OEGA	RAFT	AIBN	OEGA Conversion (%)	DP_{NMR}	$M_{n,\,NMR}$ (kg mol^{-1})	DP_{th}	$M_{n,\,th}$ (kg mol^{-1})	$M_{n,\,GPC}$ (kg mol^{-1})	$Đ$
$POEGA_{19}$	22	1	0.1	85	22	10.9	19	9.3	10.4	1.16
$POEGA_{31}$	40	1	0.1	77	35	17.1	31	15.2	15.1	1.21
$POEGA_{51}$	70	1	0.1	73	71	34.4	51	24.3	19.7	1.28

molecular weight, the hydrophilic-to-lipophilic balance (HLB) values were calculated according to the Griffin equation:[31]

$$\mathrm{HLB} = \frac{W_\mathrm{H}}{(W_\mathrm{H} + W_\mathrm{L})} \times 20 \quad (1)$$

where W_H corresponds to the weight fraction of the hydrophilic block (OEGA) and W_L corresponds to the weight fraction of the lipophilic block (4CPA and LA).

Determination of the reactivity ratios

The monomer reactivity ratios between 4CPA and LA were determined using the Jaacks method.[32] Two polymerizations were carried out, each with an excess (95 : 5) of one of the monomers, 4CPA or LA. In an exemplary synthesis, a 5 mL Schlenk flask equipped with magnetic stirrer was filled with 4CPA (200 mg, 1.315 mmol, 500 eq.), LA (15.8 mg, 0.0658 mmol, 25 eq.), $\mathrm{POEGA_{19}}$ (319 mg, 0.0343 mmol, 13 eq.), AIBN (2.6 mg, 0.0158 mmol, 6 eq.), anisole (0.327 mL), and naphthalene (10 mg, as internal standard). The mixture was degassed by sparging with nitrogen for at least 30 minutes. The flask was sealed with a nitrogen filled balloon and the polymerization was started by placing the flask in a 70 °C oil bath. The monomer conversion was followed by GC-FID, by observing the disappearance of the monomer peaks relative to the internal standard peak. The reactivity ratios were determined from the resulting Jaacks plots.

Preparation of micelles and UV cross-linking

Solvent exchange method. Block-copolymer micelles were prepared by a solvent exchange method.[33] This method was performed by dissolving the block-copolymer in an organic solvent and inducing micelle formation by slowly adding water. The procedure was as follows: a 250 mL round-bottom flask equipped with magnetic stirrer was charged with 20 mg of block-copolymer and 10 mL THF. The solution was then stirred for 20 minutes to homogenize the system. 90 mL water was added dropwise over the course of three hours with an addition rate of about 0.5 mL $\mathrm{min^{-1}}$ to induce micelle formation. The final block-copolymer concentration was 0.2 mg $\mathrm{mL^{-1}}$ in a solvent ratio $\mathrm{H_2O}$: THF of 90 : 10. To remove the remaining THF, the mixture was then dialyzed against $\mathrm{H_2O}$ in regenerated cellulose dialysis membranes with a molecular weight cut-off of 1 kDa for 24 hours. To cross-link the micelles, the colloidal solution was irradiated for 30 minutes using a 400 W metal halide, UVA lamp in a Dymax ECE 2000 UV chamber under a nitrogen flow. The distance of the lamp to the samples was 20 cm. The emitted wavelength of the lamp was in the range of UVA radiation between 350 and 450 nm.

Nanoprecipitation method. The block copolymer (20 mg) was dissolved in 10 mL THF. The solution was added dropwise to 90 mL water while stirring. The addition of the block copolymer solution was completed within 10 minutes, and the mixture was left stirring for 1 hour to homogenize the system. The mixture was dialyzed against $\mathrm{H_2O}$ in regenerated cellulose dialysis membranes with a molecular weight cut-off of 1 kDa for 24 hours. The particle size was measured on DLS to compare the nanoprecipitation method with the solvent exchange method.

Micelle loading with hydrophobic probes and doxorubicin

Loading of the micelles using the probes Nile red and pyrene was performed as follows. In a 25 mL round-bottom flask equipped with magnetic stir bar were dissolved 6 mg block copolymer and 6 mg Nile red or pyrene in 1 mL THF. The solution was thoroughly homogenised for 30 minutes and then 9 mL deionised water was added drop-wise over the course of about 1 hour. The solids were filtered over 2–3 μm filtration paper. Prior to characterization with UV-Vis, 2 mL of the Nile red loaded micelles was lyophilized and the remaining solids were dissolved in 2 mL methanol. For the pyrene loaded micelles, 200 μL of the colloidal solution was diluted in 3800 μL methanol.

To produce the DOX loaded micelles, 40 mg DOX-HCl was dissolved in 10 mL DMSO and to that 30 μL TEA was added to produce the hydrophobic form of DOX. The mixture was stirred for 1 hour and then 100 mg of the block copolymer $\mathrm{POEGA_{19}}$-$\mathrm{HB_{50}}$ was added. After thorough homogenisation, 90 mL water was added dropwise over the course of 1 hour. The precipitated DOX was filtered over a 2–3 μm paper filter and the loaded micelles were dialyzed against water (using regenerated cellulose dialysis membranes with a molecular weight cut-off of 1 kDa) to remove the DMSO.

The concentration of loaded compound was determined, after correcting for the dilutions, with UV-Vis spectroscopy by comparing the measured absorptions to a calibration curve. The drug loading content (DLC) and Encapsulation Efficiency (EE) were calculated as follows:

$$\mathrm{DLC} = \frac{\text{Weight of encapsulated model drug}}{(\text{Weight of encapsulated model drug} + \text{weight of block copolymer})} \times 100\% \quad (2)$$

$$\mathrm{EE} = \frac{\text{Weight of encapsulated model drug}}{\text{Weight of model drug in feed}} \times 100\% \quad (3)$$

Characterization

Nuclear magnetic resonance (NMR) spectroscopy. Structural characterization and OEGA monomer conversion determination was performed using ^{1}H NMR spectroscopy. ^{1}H NMR (300 MHz) spectra were recorded on a Bruker Avance III HD Nanobay 300 MHz apparatus at 298K and with 16 scans. The polymers were dissolved in $\mathrm{CDCl_3}$ or $\mathrm{D_2O}$. OEGA conversion was determined by following the disappearance of OEGA acry-

late group resonances relative to trioxane as the internal standard, which was added at the beginning of the polymerization.

Diffusion-Ordered NMR (DOSY) spectra were recorded on a Bruker Avance III HD 700 MHz spectrometer at 298K. The polymers were dissolved in $CDCl_3$. Delays of big delta and little delta were set to 50 ms and 5 ms, respectively. 8 scans were averaged for each collected FID and diffusion profiles were sampled over 32 gradient power levels selected linearly between 2% and 98% of the maximum spectrometer gradient strength. Recorded pseudo 2D diffusion data were processed in DOSY2d mode, and diffusion coefficients D (m^2 s^{-1}) were fitted using (mono) exponential fitting of spectral proton resonance lines in intensity mode.

Gas chromatography with flame ionization detection (GC-FID). GC-FID measurements were performed on a Shimadzu GC-2010 equipped with a Supelco SPB-1 capillary column (30 m × 0.25 mm × 0.25 μm film thickness). GC-FID was used to follow the disappearance of the individual monomers in the copolymerizations relative to naphthalene as the internal standard, which was added at the beginning of the polymerization. The temperature program was as follows: an initial temperature of 80 °C was maintained for 3 min and then increased to 140 °C with a heating rate of 10 °C min^{-1}. This temperature was maintained for 1 min and further increased to 300 °C with a heating rate of 20 °C min^{-1} and was maintained at 300 °C for 5 min (the total run time of 23 min).

Gel permeation chromatography (GPC). GPC was used to determine the molar mass and the dispersity. Approximately 5 mg of polymer was dissolved in 1.5 mL of dimethylformamide containing 6 g L^{-1} AcOH and 0.035 mol L^{-1} LiCl. The solution was filtered over a 0.2 μm Teflon syringe filter. The polymer solutions were then measured on a Waters GPC at 40 °C. DMF containing 6 g L^{-1} AcOH and 0.035 mol L^{-1} LiCl was used as the eluent. Three columns (Styragel HR4, Styragel HR2, and Styragel HR0.5) including a guard column were used. For the calibration curve, poly(methyl methacrylate) standards with a molar mass ranging from 800 to 2 200 000 g mol^{-1} were used.

Differential scanning calorimetry (DSC). The isolated unmodified and cross-linked micelles were measured on a Netzsch DSC 214 Polyma instrument. Prior to measurement, the samples were dried at 40 °C in a vacuum oven. The samples were heated in 2 cycles under nitrogen atmosphere from −40 °C to 100 °C with a rate of 10 °C min^{-1}. The second cycle was used for determination of the phase transition points.

UV-Vis spectroscopy. UV-Vis measurements were performed on a Shimadzu UV-3600 UV-Vis-NIR spectrophotometer using quartz cuvettes. The spectra were recorded from 800 to 200 nm with a slit width of 1 nm. Changes in absorptions of the pyrene and Nile red solutions in methanol were recorded at 334 and 552 nm, respectively. The presence DOX in water was recorded at 482 nm.

Dynamic light scattering (DLS). The size distribution of the block copolymer assemblies was determined using DLS. The aqueous colloidal solutions prepared *via* the solvent exchange method were measured directly without dilution. The block copolymers that were directly dissolved in water were measured at the same concentration of the micelles prepared *via* the solvent exchange method, which was 0.2 mg mL^{-1}. The samples were measured on a Malvern Instruments Zetasizer Nano ZS DLS instrument at 25 °C and a fixed angle of 173°.

Cryogenic transmission electron microscopy (Cryo-TEM). The block copolymer assemblies were visualized by Cryo-TEM. The block copolymer assemblies were concentrated to a concentration of 5 mg mL^{-1}. A thin aqueous film was formed by applying a 5 μl droplet of the suspension to a bare specimen grid. Glow-discharged holey carbon grids were used. After the application of the suspension, the grid was blotted against filter paper, leaving thin sample film spanning the grid holes. These films were vitrified by plunging the grid into ethane, which was kept at its melting point by liquid nitrogen, using a Vitrobot (Thermo Fisher Scientific Company, Eindhoven, Netherlands) and keeping the sample before freezing at 95% humidity. The vitreous sample films were transferred to a Tecnai Arctica cryo-electron microscope (Thermo Fisher Scientific, Eindhoven, Netherlands). Images were taken at 200 kV with a field emission gun using a Falcon III direct electron detector.

Matrix-assisted laser desorption/ionization time-of-flight mass spectroscopy (MALDI-ToF-MS). MALDI-ToF-MS spectra were recorded on a Bruker UltrafleXtreme spectrometer with a 355 nm Nd:Yag laser (2 kHz repetition pulse/Smartbeam-II) and a grounded steel plate. DCTB was used as the matrix (20 mg mL^{-1} in THF), and KTFA was used as a cationization agent (10 mg mL^{-1} in THF). The polymers were dissolved in THF (10 mg mL^{-1}). Solutions of the matrix, salt, and polymer were mixed in volume ratios of 200 : 10 : 30, respectively. All mass spectra were recorded in the linear mode. Poly(ethylene glycol) standards with M_n of 5000, 10 000, and 15 000 g mol^{-1} were used for calibration. mMass was used to process the data.

Surface tension. The surface tension was determined by the pendant drop method using an Attension Theta optical tensiometer. Block copolymer solutions with known concentration were prepared in Milli-Q water. The surface tension was calculated by the One Attension analysis software from the shape of the drop (5 μL) using the Young-Laplace equation. The concentration range that was evaluated was between 5×10^{-5} and 8×10^{-2} mM. The critical aggregation concentration (CAC) was calculated at the intersection of the tangent lines of the linear region and the plateau.

Gel content. Gel content measurements were performed on the cross-linked and unmodified micelles. Excess H_2O of both micellar solutions was evaporated in a rotary evaporator to a final micelle concentration of about 1.5 mg mL^{-1}. A paper filter was accurately weighed (W_1) and the micelle solution was added dropwise, and was allowed to dry overnight (W_2). The filter was then extracted in a Soxhlet setup using THF for 24 hours, and dried overnight (W_3) in a 40 °C vacuum oven.

The gel content measurements were performed in triplex. The gel content was calculated as follows:

$$\text{Gel content} = \frac{(W_3 - W_1)}{(W_2 - W_1)} \times 100\% \quad (4)$$

***In vitro* release of DOX.** The *in vitro* release of DOX from the unmodified and cross-linked micelles was performed in a PBS buffer with a pH of 7.4, and a sodium acetate buffer with a pH of 5.0. For the release experiment, 5 mL of the DOX loaded micelles was transferred to a dialysis bag with a molecular weight cut-off of 1 kDa. The dialysis bag was the submersed in 100 mL of the buffer and the mixture was gently stirred at 100 rpm. After several time intervals, 2 mL of the dialysis liquid was taken and replaced with 2 mL of the fresh buffer. The samples were analyzed using UV-Vis to determine the DOX concentration.

***In vitro* cytotoxicity assay.** The cytotoxicity was evaluated by measuring cell metabolic activity by a PrestoBlue® assay, which is a good indicator of cell viability. Two types of cells were used, L929 fibroblast cell line from mouse for the evaluation of the non-loaded micelles and MDA-MB-231 human cell line of breast adenocarcinoma for the evaluation of the DOX loaded micelles. The cells were obtained from ATCC. For both cell type the culture medium used was Dulbecco's Modified Eagle's Medium (DMEM, ThermoFisher) with glutamax supplemented with 1% penicillin–streptomycin and 10% fetal bovine serum (FBS).

L929 cells were seeded at 5×10^3 cell per cm^2 in 48-well plates for the pre-loading evaluation. Cells were cultured in cell culture medium during 48 h to reach subconfluence (80%). Prior to the complementation of the medium, the micelles were concentrated using evaporation to 20 mg mL^{-1} and then diluted in the cell medium to the appropriate concentration. The media was complemented with unmodified micelles, cross-linked micelles, or POEGA macro-RAFT agent. For each condition, 3 concentrations were tested: 2, 0.2, and 0.02 mg mL^{-1}. MDA-MB-231 cells were seeded at 2.5×10^4 cells per cm^2 in 48-well plates for the post-loading evaluation. Cells were cultured in the cell culture medium for 48 h to reach subconfluence (80%). Then the media was complemented with either unmodified micelles, or cross-linked micelles or free DOX. For all conditions 3 concentrations of DOX were tested: 0.1, 1, and 10 μg mL^{-1}. Untreated cell control was always included as a reference (100% cell viability).

After 72 h, the cells were incubated 30 min with PrestoBlue® solution diluted in the culture medium (1 : 9 v/v). Then supernatants were collected to measure the fluorescence (Excitation 560 nm/Emission 590 nm) using a CLARIOstar plate reader.

Results and discussion

Block copolymers consisting of POEGA as the hydrophilic block and a copolymer of 4CPA and LA as the hydrophobic block were synthesized with different POEGA and hydrophobic block lengths. For the hydrophilic block, POEGA macro-RAFT agents with a degree of polymerization of 19, 31, and 51 were used (Table 1). An overlay of the GPC traces is shown in Fig. S2.† The POEGA macro-RAFT agents were employed in a solvent polymerization to attach the hydrophobic block consisting of 30 mol% 4CPA and 70 mol% LA. Three different hydrophobic block lengths were synthesized with a targeted degree of polymerization (DP) of 20, 40, and 60, resulting in nine unique block copolymers (Table 2). Corrected for the molecular weight, these compositions result in block copolymers with a relatively large hydrophilic weight fraction and corresponding high HLB value. Block copolymer micelles containing large and dense hydrophilic shells such as provided by the nonionic POEGA possess higher stability and improved stealth properties.[24,34,35]

Block copolymer synthesis

Copolymerization of 4CPA with LA in the presence of the POEGA macro-RAFT agents proceeded without cross-linking

Table 2 Characteristics of the synthesized amphiphilic block copolymers

Polymer	Molar feed ratio[a]			Conv. 4CPA (%)	Conv. LA (%)	$M_{n,th}$[b] (kg mol^{-1})	$M_{n,NMR}$[c] (kg mol^{-1})	Molar ratio ^{1}H NMR[c]			HLB value
	4CPA	LA	AIBN					4CPA	LA	OEGA	
$POEGA_{19}$-HB_{16}	6	14	0.2	81	83	12.8	16.5	17	42	41	12.2
$POEGA_{19}$-HB_{37}	12	28	0.2	92	91	17.1	24.2	23	53	24	8.3
$POEGA_{19}$-HB_{50}	18	42	0.4	86	83	20.0	29.8	22	58	20	7.1
$POEGA_{31}$-HB_{17}	6	14	0.2	86	87	18.9	22.5	10	35	55	14.5
$POEGA_{31}$-HB_{38}	12	28	0.4	93	95	23.3	29.3	16	49	35	10.8
$POEGA_{31}$-HB_{49}	18	42	0.4	82	82	25.7	31.4	18	48	34	10.7
$POEGA_{51}$-HB_{15}	6	14	0.2	76	78	27.6	40.0	6	23	71	16.8
$POEGA_{51}$-HB_{32}	12	28	0.2	79	81	31.2	45.2	11	33	56	14.7
$POEGA_{51}$-HB_{47}	18	42	0.4	74	81	34.5	50.2	12	39	49	13.5

[a] Keeping the molar feed ratio of the macro-RAFT agent at 1. [b] Calculated as follows: $M_{n,th}$ = target DP_{4CPA} × $conv._{4CPA}$ × 152.05 + target DP_{LA} × $conv._{LA}$ × 240.39 + $MW_{th,\ POEGA\ macro\text{-}RAFT}$. [c] Calculated as follows for block copolymers synthesized with $POEGA_{19}$: $DP_{NMR,\ 4CPA} = I_{4CPA,\ 7.59\ ppm}/(I_{OEGA15,\ 3.38\ ppm}/66)$, $DP_{NMR,\ LA} = (I_{LA,\ 0.88\ ppm}/3)/(I_{OEGA15,\ 3.38\ ppm}/66)$, $M_{n,NMR} = DP_{4CPA} \times 152.05 + DP_{LA} \times 240.39 + MW_{NMR,\ POEGA19\ macro\text{-}RAFT}$. For block copolymers synthesized with $POEGA_{31}$ and $POEGA_{51}$ the integral of the OEGA resonance at 3.38 ppm was divided by 105 and 213, respectively.

that could occur as a result of side reactions on the pendent cyclopentenone units. Previous investigation of the solvent (co)polymerization of 4CPA under RAFT control, showed that by targeting a sufficiently low DP and 4CPA-to-comonomer ratio, cross-linking can indeed be avoided.[18] In the ^{1}H NMR spectrum of POEGA$_{19}$-HB$_{37}$, the resonances corresponding to the 4CPA double bond are well visible, indicating the preservation of the cyclopentenone group on the polymer backbone (Fig. 4a). According to the ^{1}H NMR spectra of the purified block copolymers, the monomer molar ratios match with the corresponding feed ratios, taking the differences in monomer conversion into account. The molar contribution of OEGA in the final structures increases as expected with increasing POEGA block length, leading to a set of amphiphilic block copolymers with HLB values between 7.1 and 16.8. In Table 2, the monomer composition and HLB values of all synthesized block copolymers is presented.

In the copolymerization with LA, 4CPA displays a very similar reactivity as shown in Fig. 2a. A similar behavior is observed in the copolymerization plot drawn from the reactivity ratios (Fig. 2b and Fig. S3a, b†). 4CPA has a slightly higher tendency to polymerize relative to LA, but the copolymerization is close to statistical, resulting in an almost random distribution of cyclopentenone units on the hydrophobic backbone. Statistical copolymerization is generally expected for *n*-alkyl acrylates,[36] and in this case indicates that the cyclopentenone double bond in 4CPA does not drastically influence the reactivity ratios.

The characterization of the block copolymers using GPC yielded inconsistent values for M_n. The obtained molecular weights were lower for the block copolymers in comparison to the macro-RAFT agent (Table S1†). Characterization of block copolymers *via* GPC, especially when the chemical or physical characteristics of the blocks differ significantly, can lead to misleading results.[37] The block copolymers presented here exhibit a stark difference in terms of hydrophobicity and functional groups between the hydrophilic and hydrophobic block. The observation of a decrease in molecular weight of the block copolymers in comparison to the macro-RAFT agent was observed before and is related to changes in block and column interaction, contraction, or collapse of the polymer coil.[37,38] Block copolymerization involving the chain extension of the POEGA macro-RAFT agents was instead confirmed *via* MALDI-ToF-MS (Fig. S4a–d†). For the block copolymers, shoulders towards higher molecular weight are observed in overlay with the corresponding macro-RAFT agent. Since the MALDI-ToF-MS technique is more sensitive towards low molecular weight compounds, the curves are not representative of the actual polymer composition. Therefore, the formation of block copolymers instead of two separate homopolymers was confirmed by diffusion ordered spectroscopy (DOSY). By comparing the DOSY spectrum of block copolymer POEGA$_{19}$-HB$_{51}$ with its corresponding macro-RAFT agent POEGA$_{19}$, the decreased diffusion coefficient value for the block copolymer is revealed (Fig. S5 and S6†). Both the hydrophobic and hydrophilic signal exhibit the same value for *D* suggesting the presence of one species with constant molar mass. Similarly, the longer macro-RAFT agent POEGA$_{31}$, shows a lower value for *D* compared to POEGA$_{19}$, reflecting the higher molecular weight of a single species (Fig. S7†).

Surface-active properties

Solutions of the POEGA macro-RAFT agents and the amphiphilic block copolymers in water significantly lowered the surface tension (Fig. 3). The observed moderate values for the surface tension are in line with what can be expected for POEGA based polymeric surfactants.[39,40] The block copolymer surface tension at the critical aggregation concentration (CAC) (γ_{CAC}) ranged between 57.2 and 59.3 mN m^{-1}. For the POEGA macro-RAFT agents the γ_{CAC} was slightly lower at 57.5, 56.6, and

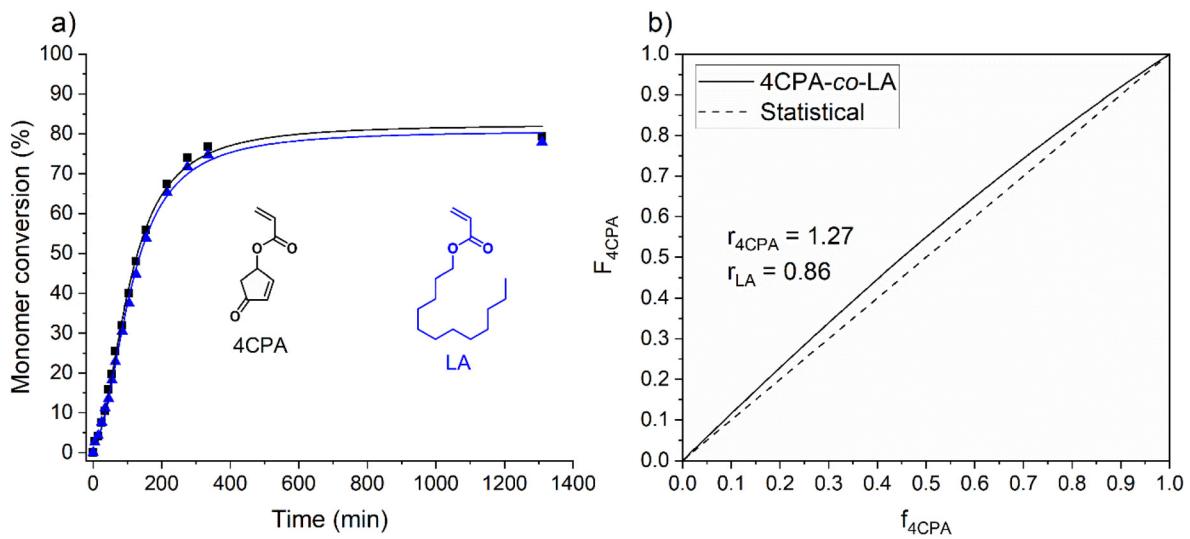

Fig. 2 (a) Monomer conversion as a function of time for the copolymerization of 4CPA (black squares) with LA (blue triangles) using macro-RAFT agent POEGA$_{19}$ (POEGA$_{19}$-HB$_{37}$). (b) Copolymerization plot of 4CPA and LA.

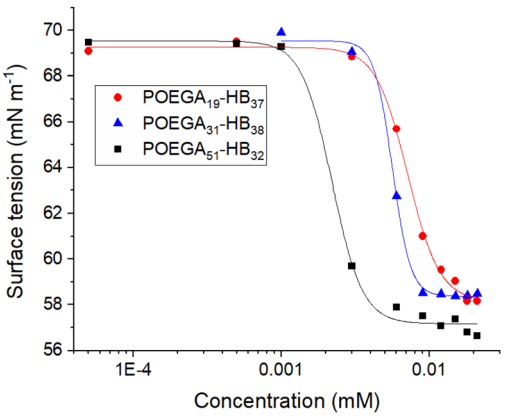

Fig. 3 Surface tension as a function of the block copolymer concentration, investigating the effect of POEGA hydrophilic block length. The calculations related to determination of the molar concentration herein are performed using the theoretical molecular weight as presented in Table 2.

55.1 mN m^{-1} for POEGA$_{51}$, POEGA$_{31}$, and POEGA$_{19}$, respectively. Surprisingly a large effect of the length of the hydrophilic block was observed, but not for the hydrophobic block (Table S2†). The CAC decreases with increasing hydrophilic block length, irrespective of the hydrophobic block length. Therefore, the CAC decrease is more likely an effect of the molecular weight increase. The lack of trend in the observed CAC values with the hydrophobic block length is opposite of the expected trend, but has been reported before with block copolymers containing complex or grafted structures.[40–42]

Self-assembly of block copolymers

The self-assembly behaviour in water of the 4CPA block copolymers was firstly demonstrated by measuring the ^{1}H NMR spectrum of the block copolymer, in this case POEGA$_{19}$-HB$_{37}$ separately in $CDCl_3$ and D_2O (Fig. 4). In $CDCl_3$, the resonances corresponding to both the hydrophilic block and the hydrophobic block are well resolved. Upon dissolution in D_2O, only the resonances corresponding to the hydrophilic POEGA block are visible (Fig. 4b). The resonances belonging to 4CPA at 7.59, 6.35, 5.83, and 2.78 ppm and LA at 4.01, 1.27, and 0.89 ppm were not visible in the spectrum. This is consistent with the self-assembly of the block copolymer into a core–shell structure with a collapsed hydrophobic core shielded by the POEGA hydrophilic shell.

Further investigation towards the self-assembly of 4CPA block copolymers was performed by DLS. Direct dissolution of the block copolymers resulted in visibly slightly turbid mixtures for the block copolymers POEGA$_{19}$-HB$_{37}$ and POEGA$_{19}$-HB$_{50}$ due to their low HLB value (<10). This is also reflected in the DLS spectra, showing typically large sizes and in some

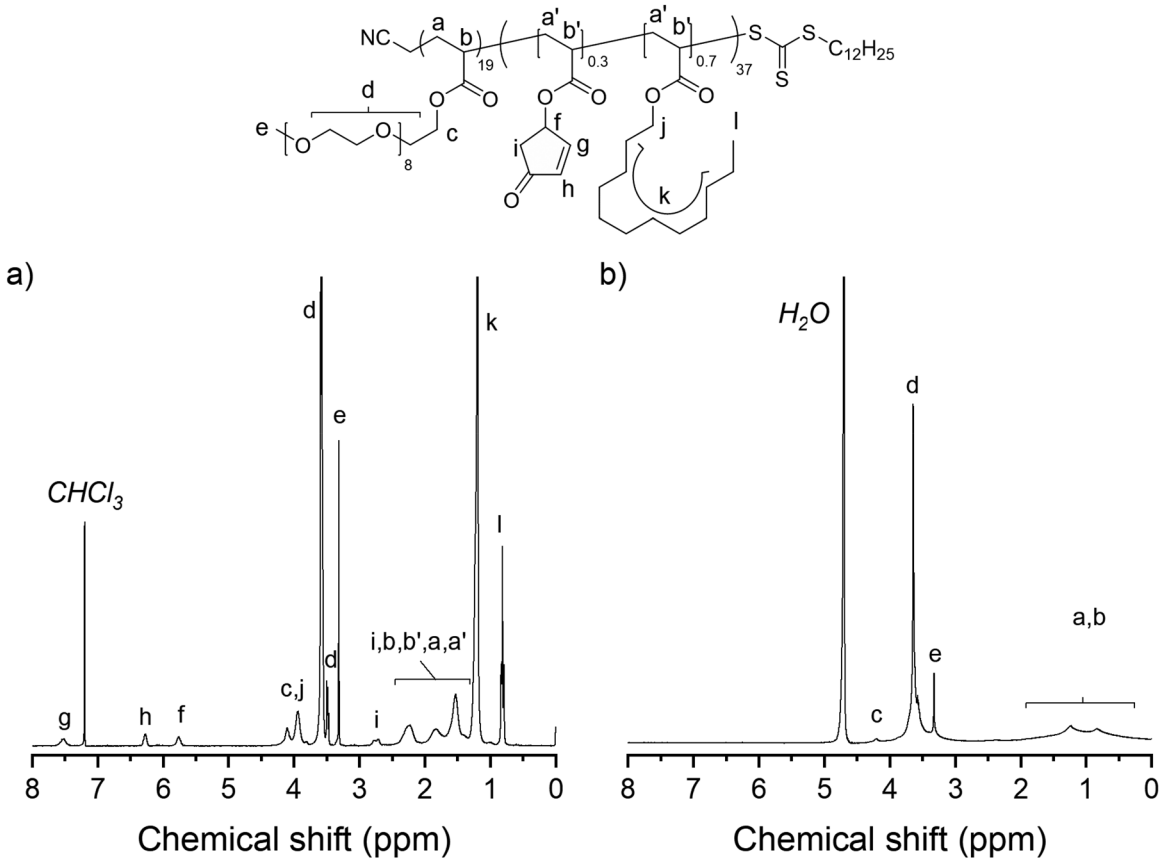

Fig. 4 ^{1}H NMR spectrum of block copolymer POEGA$_{19}$-HB$_{37}$ in (a) $CDCl_3$ and (b) D_2O.

cases a second, larger size distribution, which indicate the presence of aggregates (Table S3†). Overall, direct dissolution of the block copolymers in water resulted in a wide range of sizes of between 29 and 257 nm. In some cases, a larger micellar population was also observed. From the perspective of certain nanotechnology applications, these sizes are rather large. In the field of nanomedicine the utilization of smaller sub-100 nm micelles is favoured for the blood circulation and tissue penetration.[24] Improved performance of encapsulated drugs is observed when micelles of sub-50 nm are used due to the improved tumor tissue penetration and accumulation as a result of the enhanced permeability and retention (EPR) effect.[43–45] Furthermore, a smaller size is believed to improve the stealth properties of drug delivery vehicles, which is related to the curvature of vehicle surface.[24] Therefore, in order to attempt to reduce the size, the solvent exchange method of micelle formation was explored. Herein, the block copolymers were dissolved in an organic solvent that is a good solvent for both blocks, in this case THF. Then water is slowly added dropwise to induce micelle formation in a controlled and reproducible fashion. Remaining THF is then removed by dialysis against water. The resulting assembly dispersions were all optically clear. As a result of the solvent exchange method, in almost all cases the size was greatly reduced to sub-50 nm level (Fig. 5). The exceptions are the block copolymers with the smallest hydrophobic block length, which resulted in micelles with a size between 88 and 161 nm. Indeed, the graph shows that the hydrophobic block length strongly influences the resulting size of the micelle. The formation of micelles with a size between 29 and 40 nm is achieved for the block copolymers with intermediate hydrophobic block length. In static light scattering analysis of similar amphiphilic PEG-*block*-poly alkyl acrylate micelles with comparable molecular weight and micelle size an aggregation number of between 111 and 133 was found.[46,47] Based on the structural similarity, and comparable molecular weight and size of these POEGA block copolymer micelles, a similar aggregation number can be expected for the assemblies described here. For block copolymer $POEGA_{31}$-HB_{49}, micelles were also prepared *via* the nanoprecipitation method for comparative purposes. In this method, the block copolymer dissolved in a good solvent, in this case THF, is added dropwise to a stirring container of water, following an inverse methodology in comparison to the solvent exchange method. The resulting micelles showed a similar particle size distribution in DLS compared to the micelles obtained *via* the solvent exchange method. Particles obtained *via* the nanoprecipitation method were however, polydisperse while the particles obtained *via* the solvent exchange method are monodisperse (Fig. S8†). Therefore, the solvent exchange method is preferred.

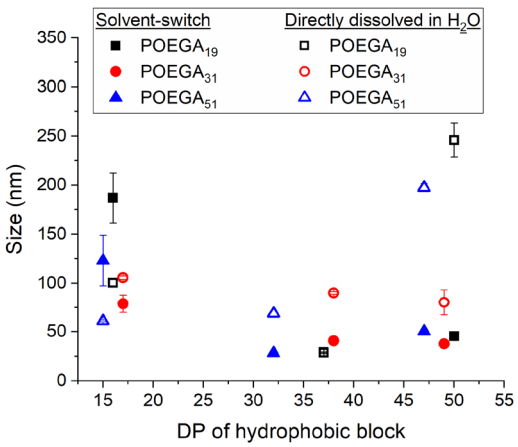

Fig. 5 Effect of the DP of the hydrophobic block for block copolymers with $POEGA_{19}$, $POEGA_{31}$, and $POEGA_{51}$ on the size measured in DLS. The sizes corresponding to two different methods of micelle formation are depicted. The solid symbols represent the solvent exchange method and the open symbols direct dissolution in H_2O.

The obtained micelles from block copolymer $POEGA_{19}$-HB_{50} were stable after storage for 4 months. No visual coagulation or sedimentation was observed and according to DLS, the sizes remained the same (Fig. S9†).

UV induced cross-linking of block copolymer micelles

Micellar structures of block copolymers bearing pendent cyclopentenone units as a part of the hydrophobic core were cross-linked using UV light. Previous research has demonstrated the UV-induced [2 + 2] photocyclodimerization of cyclopentenone side groups on a polyacrylate backbone.[18] Core cross-linking was demonstrated on the block copolymer with relatively the largest hydrophobic segment $POEGA_{19}$-HB_{50}. After self-assembly *via* the solvent exchange method, a DLS spectrum was measured to determine the initial size of the micelles, which was 36 nm (Fig. 6). A portion of the micelles was then dialyzed against THF. Replacing the aqueous medium with THF caused the micelles to dissociate and form smaller micelles of about 9 nm in diameter. Despite the solubility of the individual blocks in THF,[18] self-assembly could still occur due to the strong difference in hydrophobicity between the blocks, possibly resulting in an inverse micelle.[48] The formation of 9 nm particles in THF was confirmed separately by directly dissolving the block copolymer in THF. The same size distribution was found in DLS (Fig. 6b). The other portion of block copolymer micelles was irradiated in a UV chamber for 30 minutes. Similarly, a DLS spectrum was measured before and after dialysis against THF. In this case, the size remained the same, indicating that the micelles stayed intact due to the covalent cross-linking as a result of cyclopentenone dimerization. Another indication of the significance of cross-linking is the gel content measurement of the UV irradiated micelles. Soxhlet extraction in THF revealed a gel content of 92 ± 3%, while the unmodified micelles were completely soluble in THF. DSC spectra of the dried micelles were recorded before and after UV cross-linking (Fig. S10†). The unmodified micelles show a melting point of −12.4 °C belonging to the side chain crystals of the LA unit.[18,49] The melting peak of the cross-linked micelles is decreased to −17.1 °C and with a significantly lower melting enthalpy, caused by the disruption of crystal formation as a result of cross-linking.

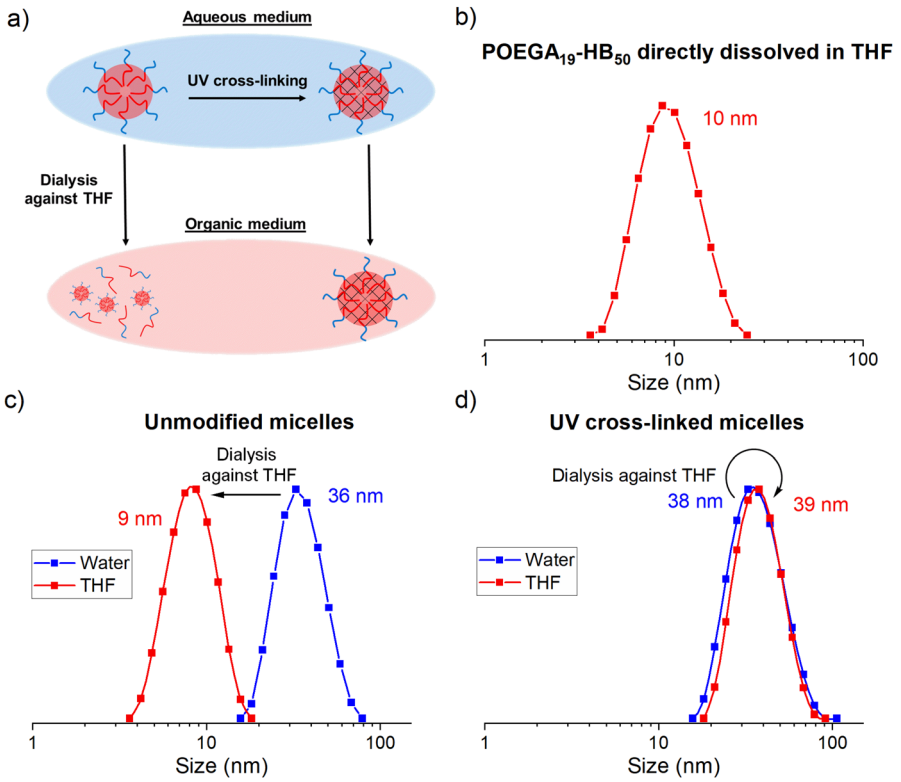

Fig. 6 DLS results of the UV cross-linked and unmodified micelles obtained from $POEGA_{19}$-HB_{50} in water and THF. (a) Schematic representation of the micelles in THF, which dissociate and form smaller micelles, but the cross-linked micelles retain their size. (b) DLS curve of $POEGA_{19}$-HB_{50} directly dissolved in THF. (c) Unmodified micelles of $POEGA_{19}$-HB_{50} before and after dialysis against THF. (d) Cross-linked micelles of $POEGA_{19}$-HB_{50} before and after dialysis against THF. The size distributions are normalized on the *y*-axis.

Unmodified and UV cross-linked block copolymer micellar assemblies from $POEGA_{19}$-HB_{37} were subjected to further characterization *via* cryo-TEM (Fig. 7b and c). As a result of changes in chemical structure and HLB value, various assembly morphologies could in theory be obtained. Generally, spherical micellar assemblies can be expected when the hydrophilic block is larger than the hydrophobic block, which is the case here.[50,51] In general, the sizes observed in cryo-TEM (Fig. 7b–d) corresponded well with those obtained from DLS (Fig. 7a). One of the benefits of core-cross-linking of block copolymer assemblies *via* external stimuli is that generally the size and shape is well maintained. Indeed, UV cross-linking did not affect the size or shape of the micelles in any way according to DLS and cryo-TEM (Fig. 7a–c). A size for the cross-linked micelles of 28 nm and 29 ± 8 nm (n = 193) is measured with the DLS and cryo-TEM, respectively. Interestingly, a very different morphology is obtained when the block copolymer is directly dissolved in water (Fig. 7d). As suggested by DLS, and confirmed by cryo-TEM, the primary size of the micelles is very small, about 29 nm. However, the assemblies have an oblong shape instead of spherical, and tend to aggregate into larger structures. According to cryo-TEM, the length average diameter is 34 ± 6 nm (n = 187) and the width average diameter is 24 ± 3 nm. Aggregation is also observed in the DLS, which shows the presence of larger micellar structures of 167 nm.

Model drug loading of block copolymers

Another benefit of the solvent exchange method is that it can be effectively combined with hydrophobic drug encapsulation to obtain block copolymer encapsulated drugs. The hydrophobic drug is simply added to the solution of block copolymer in THF, which is followed by drop-wise addition of water to induce micelle formation. In this work, the drug loading content (DLC) of all the block copolymers presented in Table 2 was investigated using two model probes, pyrene and Nile red on unmodified micelles. Both compounds are incompatible with the aqueous environment and are commonly used to probe micellar loading efficiency.[52–54] The solvent exchange method results in optically clear liquids for the pyrene loaded micelles, and in the case of Nile red encapsulated micelles, the liquid turned red (Fig. S11†). In Fig. 8a and b, the DLC is presented as a function of the DP of the hydrophobic block for the three different POEGA macro-RAFT agents. For pyrene encapsulation, a clear trend is observed. With the increase in the hydrophobic block length, the DLC increased from 0.9 to 1.8% for $POEGA_{51}$, from 1.8 to 2.7% for $POEGA_{31}$, and from 2.5 to 3.8% for $POEGA_{19}$ (Fig. 8). This shows the importance of the hydrophobic block length in block copolymer design, and suggests that pyrene persists in the hydrophobic micellar cores. The DLC's observed in this model study are rather low, but in accordance with loading values obtained for some long-

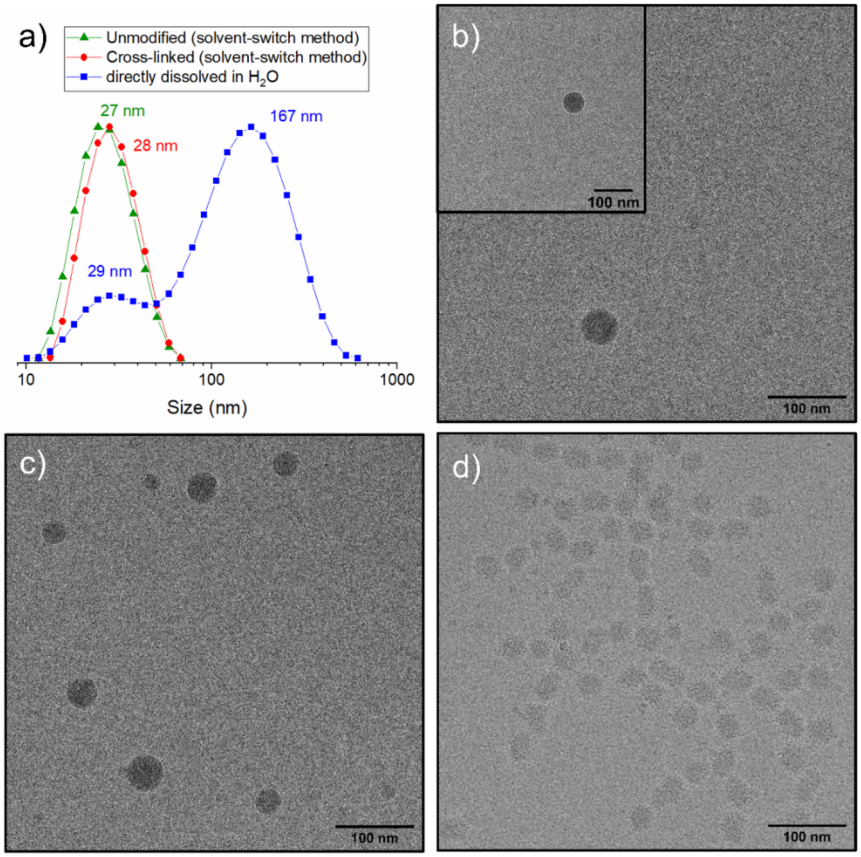

Fig. 7 Characterization of the size and shape of assemblies from block copolymer $POEGA_{19}$-HB_{37}. (a) DLS size distributions of $POEGA_{19}$-HB_{37} directly dispersed in water, and prepared *via* the solvent exchange method (unmodified and cross-linked). The size distributions are normalized on the *y*-axis. Cryo-TEM images of $POEGA_{19}$-HB_{37} block copolymer assemblies (b) unmodified (average diameter 40 ± 14 nm, *n* = 15), (c) cross-linked (average diameter = 29 ± 8 nm, *n* = 193), and (d) directly dissolved in water (length average diameter = 34 ± 6 nm, *n* = 187, width average diameter = 24 ± 3 nm, *n* = 187). Errors reported are standard deviations.

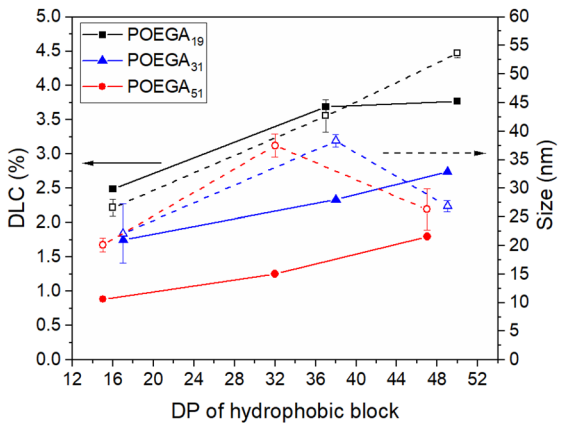

Fig. 8 Investigation of the DLC and size of the pyrene loaded micelles using DLS as a function of the DP of hydrophobic block.

chain poly alkyl acrylate amphiphilic block copolymers with various hydrophobic compounds.[55–57] Nonetheless, the loading capacity is strongly influenced by the encapsulation method.[58] In a control experiment where no block copolymer was added during the solvent exchange method, no appreciable amount of pyrene or Nile red was detected by UV-Vis (Fig. S12†). The model drug loaded micelles corresponding to all the block copolymers were colloidally stable. No pyrene or Nile red precipitation was observed during storage over several weeks.

In contrast to the pyrene encapsulation, no clear effect of the block length was observed for the DLC of Nile red loaded micelles (Fig. S13†). The DLC for the block copolymer micelles ranged between 1.1 and 2.3%. A possible explanation for the absence of effect of the block lengths on Nile red encapsulation is that Nile red can also persists in the hydrophilic PEG layer, possibly due to the presence of polar groups, that are not present in the structure of pyrene.[53]

The size and shape of polymeric micelles is influenced by the formulation parameters involved in preparing the drug loaded micelles.[2] One of them is the concentration of polymer and drugs including possible interactions between them.[59] Addition of a drug during the self-assembly can result in both smaller or larger micelles.[60,61] Therefore, the size of micelles after dye encapsulation was assessed using DLS (Fig. 8). In general, the pyrene-loaded micelles (21 to 54 nm) exhibited a

very similar size as the unmodified micelles (29 to 50 nm). The three exceptions are the block copolymers with the smallest hydrophobic block length. The size of pyrene loaded block copolymers micelles $POEGA_{19}$-HB_{16}, $POEGA_{31}$-HB_{17}, and $POEGA_{51}$-HB_{15} were reduced drastically compared to the unmodified micelles. The initial size of between 88 and 161 nm was reduced to between 21 and 30 nm. The presence of pyrene and the interactions with the hydrophobic block can influence the micellar formation process, favouring smaller micelles.

Another interesting observation is the drastic increase in size for some of the Nile red loaded micelles (Fig. S13†). This was observed for the block copolymers with a relatively large POEGA fraction. These are $POEGA_{19}$-HB_{16}, $POEGA_{31}$-HB_{17}, $POEGA_{51}$-HB_{15}, and $POEGA_{51}$-HB_{32} and consist of 41, 55, 71, and 56 mol% POEGA, respectively (Table 2). Like pyrene, the presence of Nile red during the solvent exchange procedure could have affected the micelle formation, possibly by aggregation or fusion into larger micelles. Another possibility is the increase of the hydrophobic part of the micelle, by addition of the Nile red, affecting the self-assembly process.[62]

Doxorubicin loading and *in vitro* release

$POEGA_{19}$-HB_{50}, which showed the highest pyrene loading content, was used for the DOX loading in both the unmodified and UV cross-linked form. Similar to the pyrene loading, DOX was loaded by the solvent exchange method by dissolving the DOX together with the block copolymer in an organic solvent and inducing micelle formation by slow addition of water. Compared to pyrene, the DOX was loaded in significantly higher amounts. The drug loading content for the unmodified micelles was 23.8%, and the corresponding encapsulation efficiency was also high at 78.3%. Similarly, the UV cross-linked micelles were also loaded with DOX, which was performed after the UV curing step to avoid degradation of DOX by UV light. DOX loading of the cross-linked micelles resulted in a DLC of 3.4%. The absence of the self-assembly process accompanying the DOX loading for unmodified micelles could explain the reduced loading efficiency for the UV cross-linked micelles. The photograph in Fig. S14† of the DOX loaded micelles displays the transparent and red colored solutions, indicating successful DOX encapsulation. The average size of the DOX loaded micelles was determined by DLS was 156 nm for the unmodified micelles and 84 nm for the cross-linked micelles.

The *in vitro* release of DOX from the micelles was tested at a pH of 7.4 and 5.0 (Fig. 9). The DOX release is fast initially and the release rate decreases after about 24 hours, after which only a slow increase in the cumulative DOX release is observed. For both the unmodified and cross-linked micelles, the DOX release was significantly faster at a pH of 5.0 in contrast to 7.4. While initially the release rate of the unmodified and cross-linked micelles is similar, a significant difference in the DOX release was observed after 72 hours. For the unmodified micelles, 50% of DOX was released at a pH of 5.0. The cross-linked micelles showed a significantly lower release of 31% after 72 hours. Possible incorporation of comonomers improving the interaction of DOX with the micellar vehicle *via* π–π interactions or reversible covalent bonds could further delay the initial fast DOX release rate.[63]

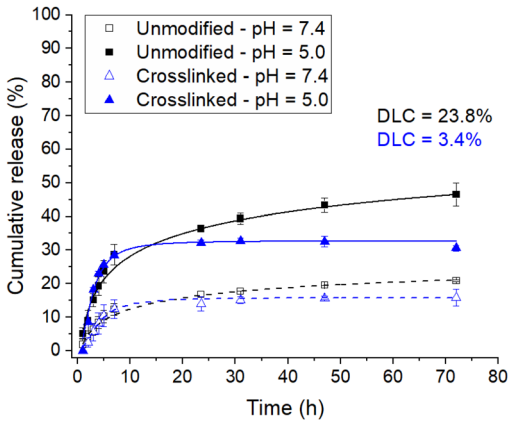

Fig. 9 Cumulative DOX release in medium of pH = 7.4 and pH = 5.0 from block copolymer micelles of $POEGA_{19}$-HB_{50}.

Cell viability

Cytotoxicity of the $POEGA_{19}$-HB_{50} unmodified and UV cross-linked micelles was tested with healthy L929 mouse fibroblast cells. Both micelles were compared to the $POEGA_{19}$ macro-RAFT agent, which showed low cytotoxicity (Fig. 10a).[26] The cells showed higher viability with low concentrations of micelles, similar to the POEGA macro-RAFT agent. However, at an elevated concentration of 2 mg mL^{-1}, low to zero cell viability was observed for the micelles, whereas POEGA showed cell viability of around 50%. The cells morphology, round instead of elongated, support the previous observation on the cytotoxic effect (Fig. S15†). At concentrations above 0.2 mg mL^{-1}, the cross-linked micelles showed a higher cytotoxicity compared to the unmodified micelles. This could possibly be caused by the evolution of small molecules as a result of the UV irradiation due to homolytic cleavage or hydrolysis reactions of the ester groups.

The same micelles from $POEGA_{19}$-HB_{50} loaded with DOX, were tested on MDA-MB-231 breast adenocarcinoma cells at a DOX concentration of 0.1, 1, and 10 μg mL^{-1}. The cell viability was compared with free DOX-HCl. In the graph in Fig. 10b, the cell viability as a function of the DOX concentration is shown. The DOX loaded micelles clearly had an impact on cell viability, a decrease of cell viability was observed demonstrating a cytotoxic effect. This effect is also illustrated by cell morphology (Fig. S16†), many round cells were observed. Plus, at high concentrations, many dead cells were noticed (Fig. S16†). The cell viability also decreases with increasing DOX concentration. The cell viability is reduced to below 20% in all cases at a DOX concentration of 10 μg mL^{-1} after 72 hours, indicating the cytotoxic effect of DOX on the MDA-MB-231 cells. Interestingly, higher cell viability was observed with the cross-linked micelles, at all instances compared to the free DOX-HCl and unmodified micelles. This result indicates a delayed exposure of the DOX to the cells, as suggested by the previous

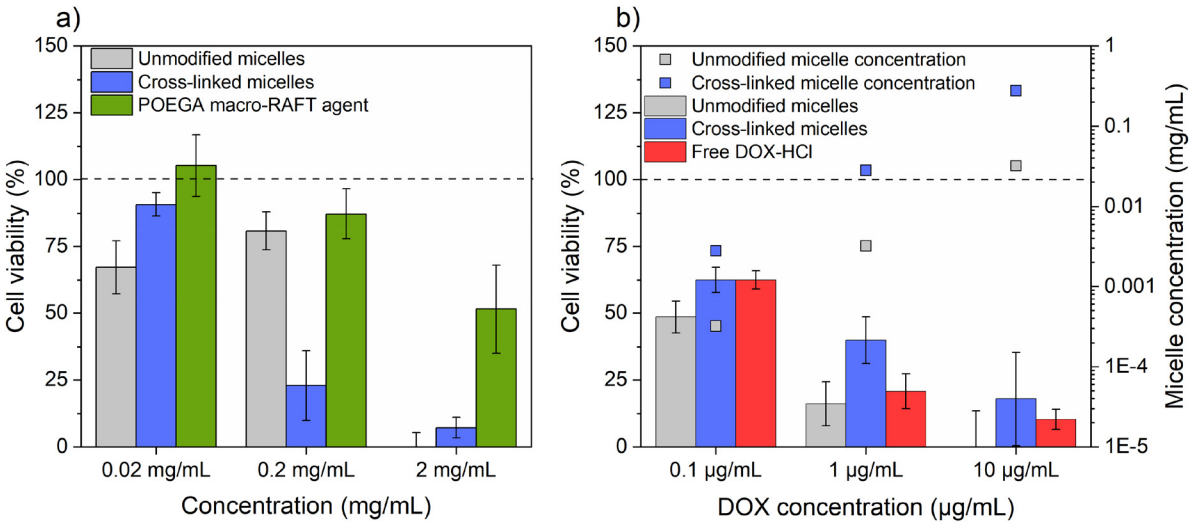

Fig. 10 (a) Cell viability of L929 cells in the presence of various concentrations of unmodified and cross-linked micelles, and POEGA macro-RAFT agent after 72 hours exposure. (b) Cell viability of MDA-MB-231 cells in the presence of various concentrations of DOX loaded unmodified and cross-linked micelles, and free DOX-HCl after 72 hours exposure.

results (Fig. 9). Furthermore, the DOX loaded micelles showed cytotoxicity towards MDA-MB-231 cells at a concentration of micelles that is not cytotoxic towards the L929 cells (*i.e.* below 0.2 mg mL^{-1}). Optimizations in DOX loading and block copolymer design could improve the cytotoxic effect of DOX against breast adenocarcinoma cells.

Conclusions

In this work, we successfully synthesized UV cross-linkable amphiphilic block copolymers containing cyclopentenone side groups on the hydrophobic backbone. Utilizing RAFT controlled copolymerization with POEGA as the hydrophilic block, 4CPA and LA readily copolymerized to form the hydrophobic block. In this way, a series of block copolymers exhibiting various block lengths and ratios were synthesized and further investigated. According to ^{1}H NMR spectroscopy, the cyclopentenone double bond remained intact during polymerization, which is required for the possibility of dimerization under UV-light to obtain core cross-linked micelles.

Self-assembly of block copolymers in water was demonstrated by ^{1}H NMR spectroscopy, DLS, and cryo-TEM. Preparation of the assemblies *via* a solvent exchange method yielded smaller and more defined spherical micelles compared to direct dissolution in H_2O. As shown for block copolymer $POEGA_{19}$-HB_{37}, it formed oblong micelles as part of a larger aggregated structure. The size of the micelles prepared by the solvent exchange method was also strongly influenced by changes in hydrophobic block length. Especially medium to long hydrophobic blocks led to sub 50 nm micelles. The hydrophilic block length also influenced the surface tension properties of the block copolymers. All macro-RAFT agents and block copolymers significantly reduced the surface tension above the CAC.

The synthesized block copolymers were successfully loaded with model drugs. In here, the solvent exchange method was easily combined with model drug loading, by simply dissolving the model drug together with the block copolymer prior to water addition. This was demonstrated using the probes pyrene and Nile red. The best loading capacities were obtained for pyrene with block copolymer containing the relatively largest hydrophobic blocks, suggesting that pyrene persists in the micellar cores. Compared to unmodified micelles, the size of pyrene-loaded micelles remained similar (<50 nm), or was drastically reduced in some cases. The small size is a requirement for potential use as drug delivery devices in nanomedicine applications. The results from the micellar probe experiments were used to load the micelles with the cancer therapeutic drug, doxorubicin at a high drug loading content of 23.8%. The micelles showed a pH dependent release of the DOX, indicating the efficacy in therapeutic applications where inclusion in the acidic environment of the intracellular organelles *via* endocytosis is the mode of micellar uptake. L929 cells showed a good cell viability in presence of the micelles, proving the low cytotoxicity of the developed drug vehicles. The micelles are effective vehicles for the hydrophobic DOX as indicated by *in vitro* cell viability tests with breast carcinoma MDA-MB-231 cell line.

Conflicts of interest

The authors declare no conflict of interest.

Acknowledgements

L. M. and J. B. acknowledge the support of European Union's Horizon 2020 research and innovation program under grant

agreement no. 953169 (Interlynk). J. S., N. S., and K. V. B. acknowledge the project D-NL-HIT carried out in the framework of INTERREG-Program Deutschland-Nederland, which is co-financed by the European Union; the MWIDE NRW; the Ministerie van Economische Zaken en Klimaat; and the provinces of Limburg, Gelderland, Noord Brabant, and Overijssel. The authors would like to thank Carmen López-Iglesias and Hans Duimel from the Microscopy CORE Lab (Maastricht Multimodal Molecular Imaging Institute (M4I)), for performing the cryo-TEM imaging at a reduced fee, as well as their advice on the data interpretation. The authors acknowledge Ryan van Zandvoort and Luc Leufkens from TNO at the Brightlands Chemelot site in Geleen for using the DLS instrument in their lab and thank Luc Leufkens for assisting with DLS measurements and data interpretation.

References

1 H. Cabral, K. Miyata, K. Osada and K. Kataoka, Block copolymer micelles in nanomedicine applications, *Chem. Rev.*, 2018, **118**(14), 6844–6892.
2 Y. Lu, E. Zhang, J. Yang and Z. Cao, Strategies to improve micelle stability for drug delivery, *Nano Res.*, 2018, **11**(10), 4985–4998.
3 W. Xu, P. Ling and T. Zhang, Polymeric micelles, a promising drug delivery system to enhance bioavailability of poorly water-soluble drugs, *J. Drug Delivery*, 2013, **2013**, 340315.
4 E. S. Read and S. P. Armes, Recent advances in shell crosslinked micelles, *Chem. Commun.*, 2007, (29), 3021–3035.
5 G. Gaucher, M.-H. Dufresne, V. P. Sant, N. Kang, D. Maysinger and J.-C. Leroux, Block copolymer micelles: preparation, characterization and application in drug delivery, *J. Controlled Release*, 2005, **109**(1–3), 169–188.
6 C. Chen, C. H. Yu, Y. C. Cheng, H. Peter and M. K. Cheung, Biodegradable nanoparticles of amphiphilic triblock copolymers based on poly (3-hydroxybutyrate) and poly (ethylene glycol) as drug carriers, *Biomaterials*, 2006, **27**(27), 4804–4814.
7 R. K. O'Reilly, C. J. Hawker and K. L. Wooley, Cross-linked block copolymer micelles: functional nanostructures of great potential and versatility, *Chem. Soc. Rev.*, 2006, **35**(11), 1068–1083.
8 S.-i. Yusa, M. Sugahara, T. Endo and Y. Morishima, Preparation and characterization of a pH-responsive nanogel based on a photo-cross-linked micelle formed from block copolymers with controlled structure, *Langmuir*, 2009, **25**(9), 5258–5265.
9 M. Sandholzer, S. Bichler, F. Stelzer and C. Slugovc, UV–induced crosslinking of ring opening metathesis block copolymer micelles, *J. Polym. Sci., Part A: Polym. Chem.*, 2008, **46**(7), 2402–2413.
10 J. Jiang, B. Qi, M. Lepage and Y. Zhao, Polymer micelles stabilization on demand through reversible photo-crosslinking, *Macromolecules*, 2007, **40**(4), 790–792.
11 J. He and Y. Zhao, Light-responsive polymer micelles, nano-and microgels based on the reversible photodimerization of coumarin, *Dyes Pigm.*, 2011, **89**(3), 278–283.
12 Y. Shi, R. M. Cardoso, C. F. Van Nostrum and W. E. Hennink, Anthracene functionalized thermosensitive and UV-crosslinkable polymeric micelles, *Polym. Chem.*, 2015, **6**(11), 2048–2053.
13 Y. Chen, A. E. Tavakley, T. M. Mathiason and T. A. Taton, Photocrosslinked poly (vinylbenzophenone)–core micelles via mild Friedel–Crafts benzoylation of polystyrene amphiphiles, *J. Polym. Sci., Part A: Polym. Chem.*, 2006, **44**(8), 2604–2614.
14 M. Nardi, T. Scherer, L. Yang, C. Kübel, C. Barner-Kowollik and E. Blasco, Stabilizing self-assembled nano-objects using light-driven tetrazole chemistry, *Polym. Chem.*, 2021, **12**(11), 1627–1634.
15 G. Kaur, S. L. Chang, T. D. Bell, M. T. Hearn and K. Saito, Bioinspired core–crosslinked micelles from thymine–functionalized amphiphilic block copolymers: Hydrogen bonding and photo–crosslinking study, *J. Polym. Sci., Part A: Polym. Chem.*, 2011, **49**(19), 4121–4128.
16 A. L. Barbarini, D. A. Estenoz and D. M. Martino, Crosslinkable micelles from diblock amphiphilic copolymers based on vinylbenzyl thymine and vinylbenzyl triethylammonium chloride, *J. Appl. Polym. Sci.*, 2015, **132**(19), 41947.
17 G. Pasparakis and M. Vamvakaki, Multiresponsive polymers: nano-sized assemblies, stimuli-sensitive gels and smart surfaces, *Polym. Chem.*, 2011, **2**(6), 1234–1248.
18 J. Stouten, D. E. Vanpoucke, G. Van Assche and K. V. Bernaerts, UV-Curable Biobased Polyacrylates Based on a Multifunctional Monomer Derived from Furfural, *Macromolecules*, 2020, **53**(4), 1388–1404.
19 K. Ulbrich, P. Kreitmeier and O. Reiser, Microwave-or microreactor-assisted conversion of furfuryl alcohols into 4-hydroxy-2-cyclopentenones, *Synlett*, 2010, 2037–2040.
20 G. Arcile, J. Ouazzani and J.-F. Betzer, Efficient Piancatelli rearrangement on a large scale using the Zippertex technology under subcritical water conditions, *React. Chem. Eng.*, 2022, 1640–1649.
21 D. J. Keddie, A guide to the synthesis of block copolymers using reversible-addition fragmentation chain transfer (RAFT) polymerization, *Chem. Soc. Rev.*, 2014, **43**(2), 496–505.
22 K. Parkatzidis, H. S. Wang, N. P. Truong and A. Anastasaki, Recent developments and future challenges in controlled radical polymerization: a 2020 update, *Chem*, 2020, **6**(7), 1575–1588.
23 N. Corrigan, K. Jung, G. Moad, C. J. Hawker, K. Matyjaszewski and C. Boyer, Reversible-deactivation radical polymerization (Controlled/living radical polymerization): From discovery to materials design and applications, *Prog. Polym. Sci.*, 2020, **111**, 101311.
24 A. Vonarbourg, C. Passirani, P. Saulnier and J.-P. Benoit, Parameters influencing the stealthiness of colloidal drug delivery systems, *Biomaterials*, 2006, **27**(24), 4356–4373.

25 J. F. Lutz, Polymerization of oligo (ethylene glycol)(meth) acrylates: Toward new generations of smart biocompatible materials, *J. Polym. Sci., Part A: Polym. Chem.*, 2008, **46**(11), 3459–3470.
26 D. Pissuwan, C. Boyer, K. Gunasekaran, T. P. Davis and V. Bulmus, In vitro cytotoxicity of RAFT polymers, *Biomacromolecules*, 2010, **11**(2), 412–420.
27 Ö. Azeri, D. Schönfeld, L. Noirez and M. Gradzielski, Structural control in micelles of alkyl acrylate-acrylate copolymers via alkyl chain length and block length, *Colloid Polym. Sci.*, 2020, **298**, 829–840.
28 F. Li, M. Danquah and R. I. Mahato, Synthesis and characterization of amphiphilic lipopolymers for micellar drug delivery, *Biomacromolecules*, 2010, **11**(10), 2610–2620.
29 O. Tacar, P. Sriamornsak and C. R. Dass, Doxorubicin: an update on anticancer molecular action, toxicity and novel drug delivery systems, *J. Pharm. Pharmacol.*, 2013, **65**(2), 157–170.
30 J. Gupta, D. J. Keddie, C. Wan, D. M. Haddleton and T. McNally, Functionalisation of MWCNTs with poly (lauryl acrylate) polymerised by Cu (0)-mediated and RAFT methods, *Polym. Chem.*, 2016, **7**(23), 3884–3896.
31 W. C. Griffin, Classification of surface-active agents by" HLB", *J. Soc. Cosmet. Chem.*, 1949, **1**, 311–326.
32 V. Jaacks, A novel method of determination of reactivity ratios in binary and ternary copolymerizations, *Makromol. Chem.*, 1972, **161**(1), 161–172.
33 Y. Mai and A. Eisenberg, Self-assembly of block copolymers, *Chem. Soc. Rev.*, 2012, **41**(18), 5969–5985.
34 J. Zhou, H. Yao and J. Ma, Recent advances in RAFT-mediated surfactant-free emulsion polymerization, *Polym. Chem.*, 2018, **9**(19), 2532–2561.
35 M. Vittaz, D. Bazile, G. Spenlehauer, T. Verrecchia, M. Veillard, F. Puisieux and D. Labarre, Effect of PEO surface density on long-circulating PLA-PEO nanoparticles which are very low complement activators, *Biomaterials*, 1996, **17**(16), 1575–1581.
36 K. O'Leary and D. Paul, Copolymers of poly (n-alkyl acrylates): synthesis, characterization, and monomer reactivity ratios, *Polymer*, 2004, **45**(19), 6575–6585.
37 K. Philipps, T. Junkers and J. J. Michels, The block copolymer shuffle in size exclusion chromatography: the intrinsic problem with using elugrams to determine chain extension success, *Polym. Chem.*, 2021, **12**(17), 2522–2531.
38 A. Guzik and P. Raffa, Direct synthesis via RAFT of amphiphilic diblock polyelectrolytes facilitated by the use of a polymerizable ionic liquid as a monomer, *Polym. Chem.*, 2021, **12**(38), 5505–5517.
39 P. Raffa, A. A. Broekhuis and F. Picchioni, Amphiphilic copolymers based on PEG–acrylate as surface active water viscosifiers: Towards new potential systems for enhanced oil recovery, *J. Appl. Polym. Sci.*, 2016, **133**(42), 44100.
40 P. Raffa, D. A. Z. Wever, F. Picchioni and A. A. Broekhuis, Polymeric surfactants: synthesis, properties, and links to applications, *Chem. Rev.*, 2015, **115**(16), 8504–8563.
41 J.-H. Lee, S.-W. Jung, I.-S. Kim, Y.-I. Jeong, Y.-H. Kim and S.-H. Kim, Polymeric nanoparticle composed of fatty acids and poly (ethylene glycol) as a drug carrier, *Int. J. Pharm.*, 2003, **251**(1–2), 23–32.
42 D. Peng, X. Zhang, C. Feng, G. Lu, S. Zhang and X. Huang, Synthesis and characterization of amphiphilic graft copolymers with hydrophilic poly (acrylic acid) backbone and hydrophobic poly (methyl methacrylate) side chains, *Polymer*, 2007, **48**(18), 5250–5258.
43 H. Cabral and K. Kataoka, Progress of drug-loaded polymeric micelles into clinical studies, *J. Controlled Release*, 2014, **190**, 465–476.
44 H. Cabral, Y. Matsumoto, K. Mizuno, Q. Chen, M. Murakami, M. Kimura, Y. Terada, M. Kano, K. Miyazono and M. Uesaka, Accumulation of sub-100 nm polymeric micelles in poorly permeable tumours depends on size, *Nat. Nanotechnol.*, 2011, **6**(12), 815–823.
45 L. Tang, X. Yang, Q. Yin, K. Cai, H. Wang, I. Chaudhury, C. Yao, Q. Zhou, M. Kwon and J. A. Hartman, Investigating the optimal size of anticancer nanomedicine, *Proc. Natl. Acad. Sci. U. S. A.*, 2014, **111**(43), 15344–15349.
46 A. Chroni, T. Mavromoustakos and S. Pispas, Nano-Assemblies from Amphiphilic PnBA-b-POEGA Copolymers as Drug Nanocarriers, *Polymers*, 2021, **13**(7), 1164.
47 S. Piogé, L. Fontaine, C. d. Gaillard, E. Nicol and S. Pascual, Self-assembling properties of well-defined poly (ethylene oxide)-b-poly (ethyl acrylate) diblock copolymers, *Macromolecules*, 2009, **42**(12), 4262–4272.
48 S. Garnier and A. Laschewsky, Non-ionic amphiphilic block copolymers by RAFT-polymerization and their self-organization, *Colloid Polym. Sci.*, 2006, **284**(11), 1243–1254.
49 E. F. Jordan Jr., B. Artymyshyn, A. Speca and A. Wrigley, Side–chain crystallinity. II. Heats of fusion and melting transitions on selected copolymers incorporating n–octadecyl acrylate or vinyl stearate, *J. Polym. Sci., Part A-1: Polym. Chem.*, 1971, **9**(11), 3349–3365.
50 L. Zhang and A. Eisenberg, Multiple morphologies of" crew-cut" aggregates of polystyrene-b-poly (acrylic acid) block copolymers, *Science*, 1995, **268**(5218), 1728–1731.
51 F. d'Agosto, J. Rieger and M. Lansalot, RAFT–Mediated Polymerization–Induced Self–Assembly, *Angew. Chem., Int. Ed.*, 2020, **59**(22), 8368–8392.
52 N. Karanikolopoulos, I. Choinopoulos and M. Pitsikalis, Poly {dl–lactide–b–[oligo (ethylene glycol) methyl ether (meth) acrylate)]} block copolymers. Synthesis, characterization, micellization behavior in aqueous solutions and encapsulation of model hydrophobic compounds, *J. Polym. Sci.*, 2020, **58**(11), 1582–1600.
53 I. N. Kurniasih, H. Liang, P. C. Mohr, G. Khot, J. r. P. Rabe and A. Mohr, Nile red dye in aqueous surfactant and micellar solution, *Langmuir*, 2015, **31**(9), 2639–2648.
54 B. Trappmann, K. Ludwig, M. R. Radowski, A. Shukla, A. Mohr, H. Rehage, C. Böttcher and R. Haag, A new family of nonionic dendritic amphiphiles displaying unexpected packing parameters in micellar assemblies, *J. Am. Chem. Soc.*, 2010, **132**(32), 11119–11124.

55 M. Arshad, R. A. Pradhan and A. Ullah, Synthesis of lipid-based amphiphilic block copolymer and its evaluation as nano drug carrier, *Mater. Sci. Eng., C*, 2017, **76**, 217–223.

56 P. Sarkar, S. Ghosh, R. Saha and K. Sarkar, RAFT polymerization mediated core–shell supramolecular assembly of PEGMA-co-stearic acid block co-polymer for efficient anticancer drug delivery, *RSC Adv.*, 2021, **11**(28), 16913–16923.

57 P. Laskar, B. Saha, S. K. Ghosh and J. Dey, PEG based random copolymer micelles as drug carriers: the effect of hydrophobe content on drug solubilization and cytotoxicity, *RSC Adv.*, 2015, **5**(21), 16265–16276.

58 V. P. Sant, D. Smith and J.-C. Leroux, Enhancement of oral bioavailability of poorly water-soluble drugs by poly (ethylene glycol)-block-poly (alkyl acrylate-co-methacrylic acid) self-assemblies, *J. Controlled Release*, 2005, **104**(2), 289–300.

59 J. Cheng, B. A. Teply, I. Sherifi, J. Sung, G. Luther, F. X. Gu, E. Levy-Nissenbaum, A. F. Radovic-Moreno, R. Langer and O. C. Farokhzad, Formulation of functionalized PLGA–PEG nanoparticles for in vivo targeted drug delivery, *Biomaterials*, 2007, **28**(5), 869–876.

60 C. E. Astete and C. M. Sabliov, Synthesis and characterization of PLGA nanoparticles, *J. Biomater. Sci., Polym. Ed.*, 2006, **17**(3), 247–289.

61 Y. N. Konan, R. Cerny, J. Favet, M. Berton, R. Gurny and E. Allémann, Preparation and characterization of sterile sub-200 nm meso-tetra (4-hydroxylphenyl) porphyrin-loaded nanoparticles for photodynamic therapy, *Eur. J. Pharm. Biopharm.*, 2003, **55**(1), 115–124.

62 K. Parkatzidis, N. P. Truong, M. Rolland, V. Lutz-Bueno, E. H. Pilkington, R. Mezzenga and A. Anastasaki, Transformer–Induced Metamorphosis of Polymeric Nanoparticle Shape at Room Temperature, *Angew. Chem.*, 2022, **61**(8), e202113424.

63 M. Talelli, M. Iman, A. K. Varkouhi, C. J. Rijcken, R. M. Schiffelers, T. Etrych, K. Ulbrich, C. F. van Nostrum, T. Lammers and G. Storm, Core-crosslinked polymeric micelles with controlled release of covalently entrapped doxorubicin, *Biomaterials*, 2010, **31**(30), 7797–7804.